Molecular Resonance Imaging of the CAIX expression in Mouse Mammary Adenocarcinoma Cells

Claudia Quattrociocchi , Alberto Mangia , Silvio Aime , Valeria Menchise , Daniela Delli Castelli *

Posted Date: 24 August 2023

doi: 10.20944/preprints202308.1696.v1

Keywords: MRI; Molecular Imaging; CAIX; Breast cancer; Gd-contrast agent; liposomes

Article

Molecular Resonance Imaging of the CAIX Expression in Mouse Mammary Adenocarcinoma Cells

Claudia Quattrociocchi [1], Alberto Mangia [1], Silvio Aime [2], Valeria Menchise [2] and Daniela Delli Castelli [1,*]

[1] Univ Turin, Dept Mol Biotechnol & Hlth Sci, Mol Biotechnol Ctr, I-10126 Turin, Italy; daniela.dellicastelli@unito.it

[2] CNR, Inst Biostruct & Bioimaging, Mol Biotechnol Ctr, I-10126 Turin, Italy; valeria.menchise@unito.it

* Correspondence: daniela.dellicastelli@unito.it

Abstract: The Carbonic Anidrase isoform IX (hCA IX) is one of the main player in extracellular tumor pH regulation and it is known to be overexpressed in breast cancer and other common tumors. hCA IX supports the growth and survival of tumor cells and its expression is correlated to metastasis and resistance to therapies making it an interesting biomarker for diagnosis and therapy. The aim of this work deals with the development of an MRI Imaging probe able to target the extracellular non catalytic PG domain of CAIX. For this pourpose a specific nano probe was designed by conjugating a peptidic interactor of PG domain on the surface of a liposome loaded with Gd-bearing contrast agents. Mouse Mammary Adenocarcinoma Cell Line (TS/A) were chosen as *in vitro* breast cancer model to test the developed probe. MRI results showed a high selectivity and sensitivity of the Imaging probe towards hCA IX expressing TS/A cells. This approach appears highly promising for the *in vivo* translation of a diagnostic procedure based on the targeting of hCA IX enzyme expression.

Keywords: MRI; Molecular Imaging; CAIX; breast cancer; Gd-contrast agent; liposomes

1. Introduction

Despite significant advances in therapy, breast cancer (BC) is still the second leading cause of cancer death in women [1]. This indicates that a better understanding of this multifaceted disease is needed. Recent years have witnessed the growing interest toward pH deregulation phenomena taking place at both the intracellular and extracellular tumour environment. The study of H^+ dynamics in cancer has led to a new paradigm, known as the pH-centric anticancer paradigm. Such metabolic reprogramming involves intracellular alkalinization of cancer cells associated to an extracellular microenvironmental acidosis [2,3]. The alteration of pH gradient (pHi to pHe) confers to cancer cells and tissues important advantages, such as the enhancement of their resistance to hypoxia and cancer therapy [4,5]. Among others, one of the main player in pH regulation in cancer cells is the transmembrane isoform of carbonic anhydrases (hCAs), hCAIX. This enzyme is a type I transmembrane dimeric protein consisting of an extracellular part, containing the catalytic domain and a unique proteoglycan-like (PG) domain, a transmembrane (TM) region and an intracellular (IC) tail. This protein is known to be overexpressed in breast cancer as well as in many common tumors and to play a critical role in hypoxia associated tumour acidosis [6–10].

The presence of a targetable extracellular domain and the limited expression in healthy tissues contributed to make CAIX an increasingly important biomarker for cancer diagnosis and an interesting site for the design of innovative therapies.

Indeed, many CAIX inhibitors have been developed and are currently under intense scrutiny in dedicated clinical trials [11].

 doi:10.20944/preprints202308.1696.v1

Owing to its strategic role in pH regulation, CAIX has gain a crucial role as diagnostic marker. Indeed its expression level, measured after biopsy, can help distinguishing between malignant and benign lesions in some solid tumors [12]. The possibility of visualizing the CAIX expression *in vivo*, through non-invasive imaging techniques, is a very appealing goal. An interesting imaging strategy has been reported by More et al. who developed a novel [F-18]-PET tracer based on acetazolamide, a well-known CA-IX inhibitor [13]. A related near-infrared (NIR) fluorescent dye targeting the CA IX has been proposed to visualize hypoxic regions in murine models. Its application in cancer image-guided surgeries has been discussed [14].

Whereas there are several studies investigating CAIX-targeting using Optical and Nuclear Imaging techniques, up to now, no Magnetic Resonance Imaging (MRI) approach has been reported. MRI is a technique endowed with a superior soft tissue contrast and an excellent spatial resolution. Compared with nuclear imaging techniques, MRI is less invasive because its contrast agents are not radioactive substances, however showing the same ability to deeply penetrate the biological tissues, a property that strongly hampers the approaches based on Optical Imaging. Conversely the sensitivity of MRI probes is rather low, making the ability to visualize a molecular marker *in vivo* strongly dependent on the target concentration and/or on the efficacy and the amount of contrast agent accumulated at the site. To enhance the concentration of the contrast agent delivered at the target site, an established strategy consists of the use of paramagnetic liposomes that can transport a large amount of contrast agents per single vesicle, thus amplifying the effect of the molecular recognition event [15].

Liposomes are the most biocompatible clinically approved nano-sized delivery systems [16], entrapping an aqueous core inside a phospholipidic bilayer [17]. Their structure allows both the encapsulation of active components in their aqueous core and/or the incorporation in the membrane. Moreover multifunctionalized phospholipids can be considered for the membrane formulation to prepare versatile vescicles endowed with targeting properties [18].

The development of stimulus-sensitive nanovesicles has contributed to improve the *in vivo* performance of MRI responsive agents [19]. One approach exploits the process of "quenching/de-quenching", that consists in using "silenced" probes which recover their relaxation enhancing property upon the changes in the liosomes'membrane. These "T1-quenched" nanosystems are designed to recover the signal enhancement ability following the release of vesicle's payload in response to biological events, such as pH change, liposome-protein interaction and vesicle degradation, thus allowing a sensitive *in vivo* MRI detection.

This work aimed at developing a MRI diagnostic approach to evaluate the level of expression of hCA IX in a breast cancer cell model. This objective has been pursued by designing a novel Gd-based MRI nanoprobe carrying a CAIX PG domain targeting vector on the surface and a "quenched/de-quenched" T1-contrast system able to report on the specific delivery of the cargo of MRI probes at the target site and on its successive cellular uptake.

2. Results

2.1. Probe Synthesis and characterization

The strategy of the probe design consists in functionalizing the surface of paramagnetic liposomes, loaded with Gd-HPDO3A, with a maleimide group that can be used as an anchor point for the peptide molecular vector directed toward CAIX (*scheme1*). This type of bioconjugation was chosen because it requires mild conditions, such as room temperature and pH 6.5, needed to prevent biomolecule degradation.

 doi:10.20944/preprints202308.1696.v1

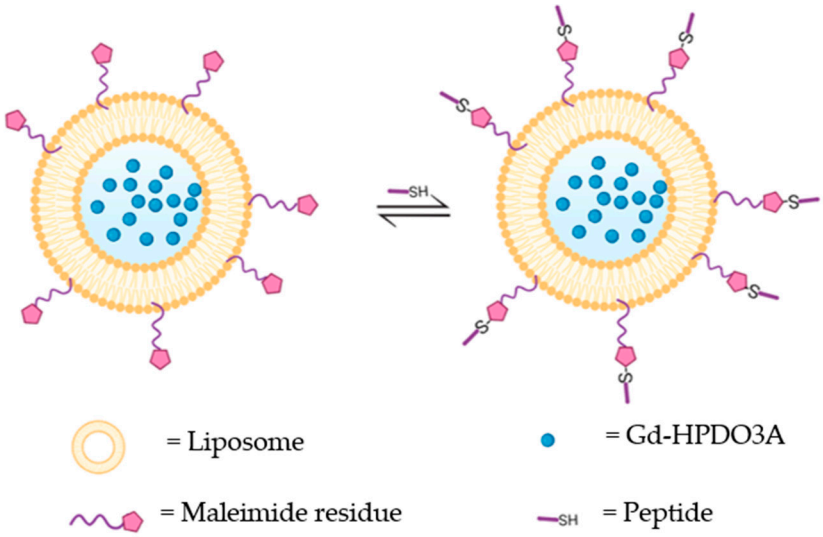

Scheme 1. Liposome loaded with Gd-HPDO3A and bioconjugated with the targetig peptide.

First we designed the amino-acid sequence of the targeting peptide to be conjugated to the nano-sized probe. The sequence was designed considering the PG domain of hCA IX as the target, since this region represents a unique feature of this enzyme being absent in all the other hCAs. Recently the crystallographic structure of the M75 antibody in complex with an epitope of the PG region [20] allowed the development of new peptides whose sequences reproduce the main Ab motifs involved in the intermolecular interaction. Extensive molecular dynamics simulations allowed to optimize the affinity of the peptides toward the enzyme targeting site. The most promising peptide developed in the study (Pep1) was chosen as a basis for the design of a peptide able to target the PG region of CAIX *via* its conjugation on the surface of a liposome. For this purpose, a cysteine residue was added to the Pep1 to introduce a free thiol group for the further conjugation to a maleimide group properly incorporated into the nano-probe external surface (see below). To improve the flexibility and the hydrophilicity of the molecule, a ASSG sequence and a PEG-based spacer were inserted before the cysteine residue. Figure 1A shows the sequence of the targeting peptide (PepC) and of the scrambled peptide (SCR) generated as a negative control. Both peptides were prepared through automated solid-phase peptide synthesis (SPPS) technique [21]. The peptide crude purities were assessed upon Ultra-performance liquid chromatography-mass spectrometry (UPLC-MS) analysis and fractions with purity higher that 90% were obtained through automated liquid chromatography system (AKTA) (Figure 1a).

Preprints (www.preprints.org) | NOT PEER-REVIEWED | Posted: 24 August 2023 doi:10.20944/preprints202308.1696.v1

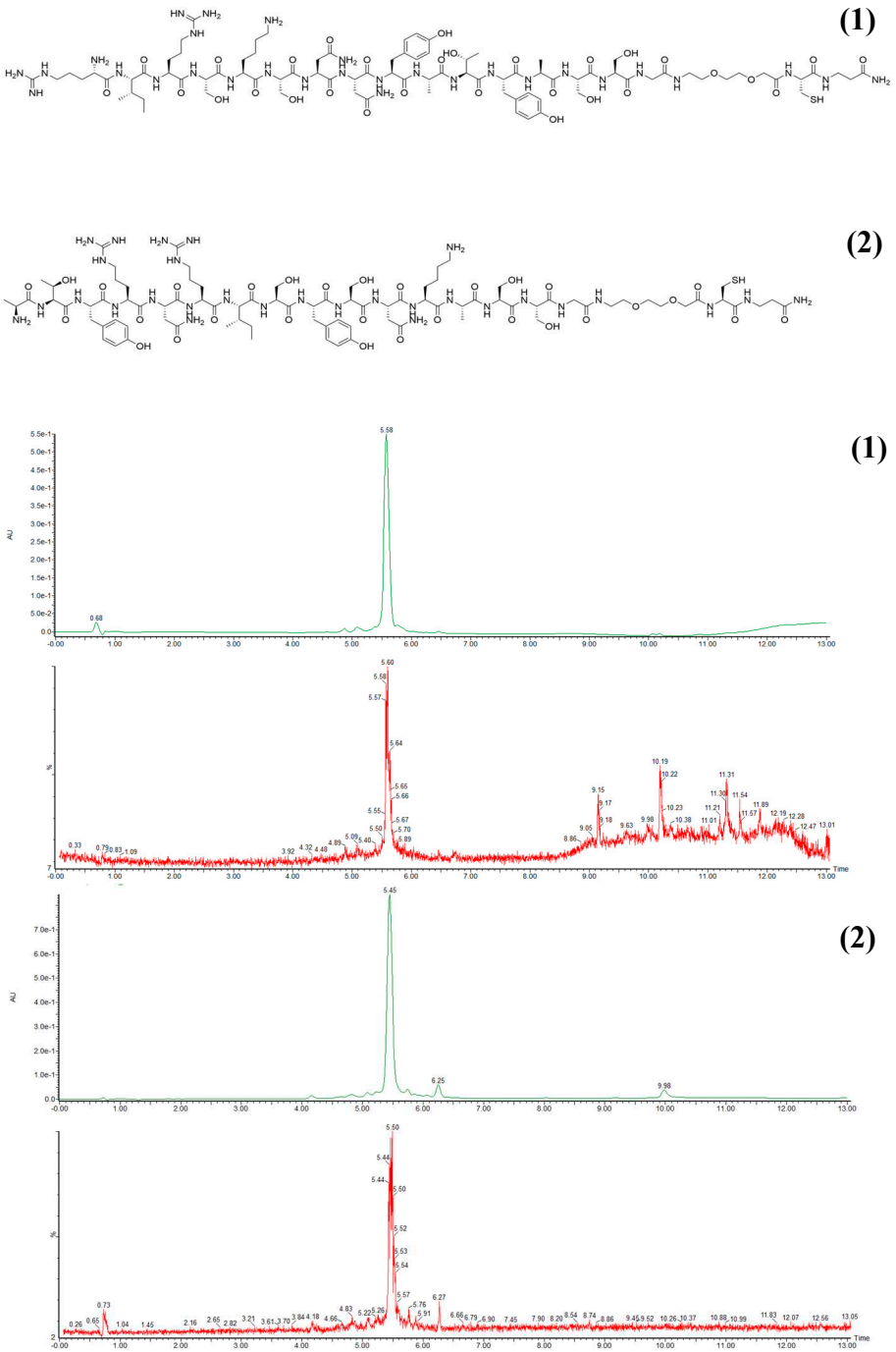

Figure 1. (**a**) Sequence of the targeting peptide (PepC) (1) and of the scramble peptide (SCR) (2); (**b**) Post-purifcation chromatograms of PepC (1) and SCR (2).

In order to prepare the paramagnetic liposomes, DPPC, DSPE-PEG 2000 MeO and DSPE-PEG 2000 Mal at 95:4:1 molar ratio were dissolved in chloroform and dried to form a thin lipidic film, that was hydrated with a 300 mM aqueous solution of the paramagnetic complex Gd-HPDO3A (ProHance). The mixture was sonicated until a suspension of liposomes with an average size of 120 nm was obtained, as measured through the dynamic light scattering method. The final suspension was allowed to react at room temperature with a stoichiometric excess of PepC to functionalize all maleimide residues present on the liposomal surface. The concentration of Gd-HPDO3A in the suspensions, as determined by NMR magnetic susceptibility measurement, allowed to estimate the concentration of the targeting liposome (LIP_PepC). A liposome functionalized with the scrambled peptide (LIP_SCR) was prepare following the same procedure. Also the unfunctionalized control

 doi:10.20944/preprints202308.1696.v1

liposome (LIP) was synthetized. It contained with DSPE-PEG 2000 in place of the DSPE-PEG 2000 Mal component.

The average size of the liposomes remained consistent with the measurement that occurred before the bioconjugation step. The size resulted to be about120 nm for all three types of probes. The final concentration of Gd-HPDO3A in the liposome suspensions was determined by NMR magnetic susceptibility measurement (Evans assay) [22], and it was found to be 4.1 mM. The relaxometric measurements, at 20 MHz and 298K, yielded, for LIP_PepC, r1p values of 0.12 mM-1 s-1 for the intact liposome and 4.7 mM-1 s-1 for the lyased liposome, respectively. For LIP_SCR, 0.13 mM-1 s-1 for the intact liposome and 4.7 mM-1 s-1 for the lyased liposome, and 0.14 mM-1 s-1 for the intact liposome and 4.7 mM-1 s-1 for the lyased liposome in the case of LIP. Determination of the total amount of Gd and the size of liposomes allowed to assess a molar concentration of liposomes of 220 nM (Materials and Methods).

2.2. MRI tests on TS/A cells

Mouse Mammary Adenocarcinoma Cell Line (TS/A) was chosen as in vitro breast cancer model to test the performance of the developed probe. This cell line is known to over-express CAIX.

The labeling experiments were designed to assess the MRI Signal Enhancement (SE) in cellular pellets at time zero (i.e. immediately after the liposomes were added to the cell suspension) and 24 h later to allow liposomes uptake from the cells via CAIX-mediated internalization. The latter experiment is intended to assess the occurrence of the intracellular de-assembly of the Liposomes, a necessary condition for detecting their MRI visualization.

The cells were incubated either with the specific targeting probe (LIP_PepC) or with the non-specific one containing the scrambled peptide (LIP_SCR) as well with the liposomes without any peptide on their surface (LIP), in order to take into account possible aspecific interactions. The final concentration of liposome in the incubation medium was 56 nM. Cells were washed with PBS and removed from plates after 4 hours of incubation at 37 °C. Cells were then transferred into 1mm capillaries and centrifuged to obtain pellets for MRI analysis. A phantom containing cell capillaries, two for each set of experimental conditions and two for unlabeled cells, was prepared and imaged at 7T micro-imager. Figure 2 displays the signal enhancement (SE) for the 8 capillaries acquired with the T1w sequence.

At time=0, i.e. immediately after the addition of the liposomes to the cell suspension, no significant difference in the observed SEs was detected for the three specimens. (Figure 2A). This could be ascribed to the fact that the liposomes, even if bound to the CAIX exposed on the cell membrane, are still intact, hence almost silent. The experiment was then acquired on specimens obtained from cells incubated at 37°C for 24 h, after the unbound probe removal (Figure 2B). This additional time had the purpose to allow liposomes to be eventually internalized and de assembled. Results clearly showed that SEs for TS/A incubated 24 hours after the probe removal were significantly larger than the ones observed at time 0. By assigning a value of 100 % to the SE observed for cells incubated with LIP_PepC , the cells incubated with LIP_SCR or LIP are at 22% and 8%, respectively (Figure 2C). This indicates a very good specificity of the LIP_PepC towards TS/A cells and also shows that this specificity yields an excellent MRI response after 24 h of incubation, i.e. when the internalized probe has released the paramagnetic molecules into the cells. ICP mass analysis of the TS/A pellets yielded a value of 1,75x10-15 moles of Gd per cell corresponding to a number of internalized liposomes per cells of 6000.

Preprints (www.preprints.org) | NOT PEER-REVIEWED | Posted: 24 August 2023 doi:10.20944/preprints202308.1696.v1

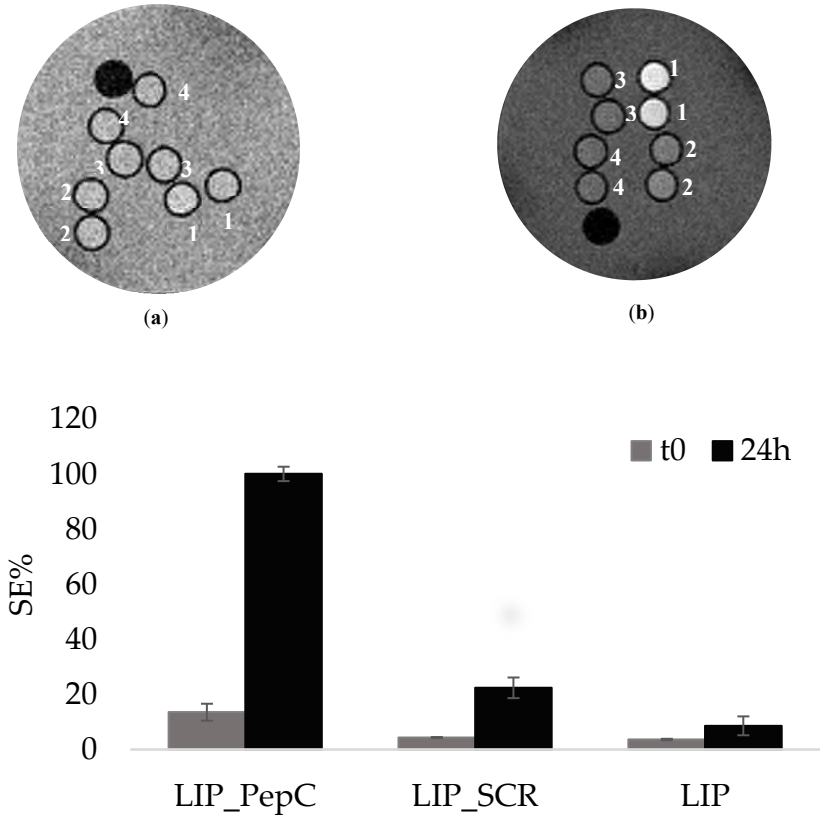

Figure 2. (a) MRI T1W of TS/A cells incubated with LIP_PepC (1), Lip_SCR(2), LIP(3) and acquired on pellets obtained from the TS/A cells immediately after the addition of the liposomes to the cell culture. (t0); (b) MRI T1W of TS/A cells incubated with LIP_PepC (1), Lip_SCR(2), LIP(3) and acquired after 24 hours of incubation (24h); Histograms showing the SEs referred to Figure 2,ab.

In order to ascertain that the specificity observed is due to CAIX targeting, a further experiment has been done comparing the SE of a specimen containing TS/A and MDA-MB-231 cells both incubated with LIP_PepC and imaged after 24h post incubation at 37°C. MDA-MB-231 cell line are known for their lower expression level of CAIX [23]. The marked difference in the observed SEs for the two cell lines clearly supports the view of the correlation between CAIX expression and signal enhancements (Figure 3A,B). Next, TS/A cells have been incubated with decreasing concentration of LIP_PEPC to test the sensitivity threshold of the targeting protocol. An enhancement of nearly 10% can still be observed for cells incubated with 7mM of LIP_PepC (Figure 4A,B).

Preprints (www.preprints.org) | NOT PEER-REVIEWED | Posted: 24 August 2023 doi:10.20944/preprints202308.1696.v1

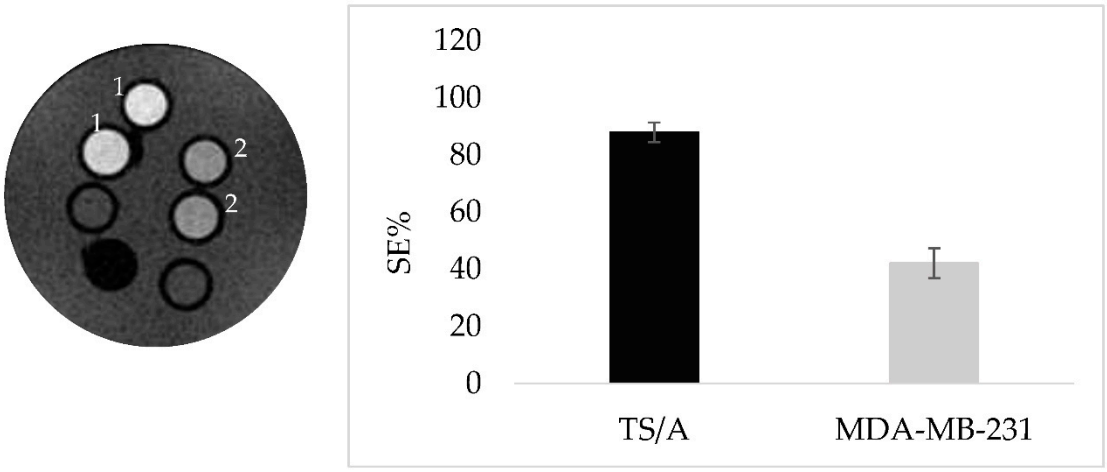

Figure 3. A (on the left) MRI T_{1W} of TS/A (1) and MDA-MB-231 (2) cells incubated with the same concentration of LIP_PepC and acquired after 24 hours. 3B Histogram showing the SE referred to Figure 3A.

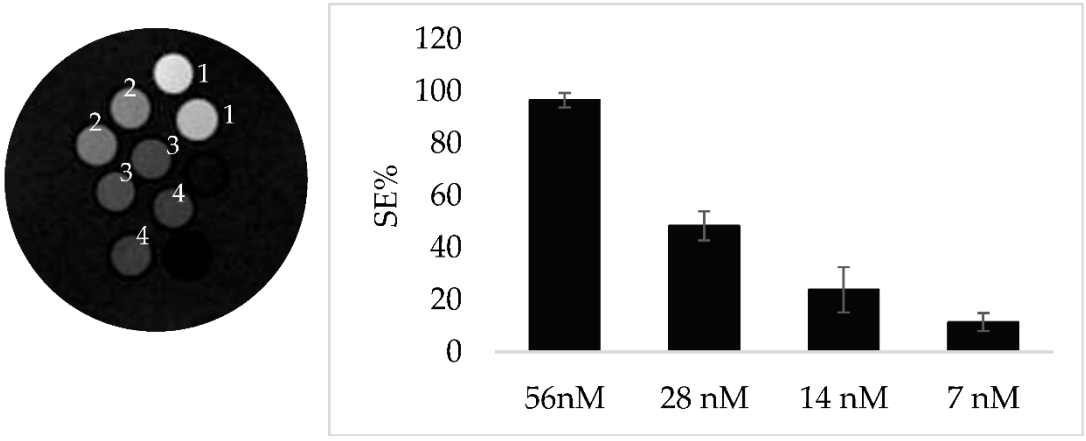

Figure 4. A MRI T_{1W} of TS/A cells incubated with different concentratios of LIP_PepC: 56nM (1), 28nM (2), 14nM (3), 7nM (4) and 4 B Histogram showing the SE referred to Figure 4A.

3. Discussion

In most solid tumors the metabolic changes necessary for the high rate of cancer cell proliferation results in alteration in intra and extracellular pH. Tumor cells overexpress proteins that can expell protons acidifying the extracellular environment (from 7.4 to 6.5-6.8) while preventing the decrease in intracellular pH that would cause cell apoptosis.

Over all, the central role played by carbonic anhydrases, in particular CAIX and CA XII, is now well established. These metalloenzymes catalyze the reversible transformation of CO2 into the bicarbonate ion with the release of a proton, thus modulating the concentration of the species required for cancer cell survival and proliferation. In recent years, carbonic anhydrases IX and XII have thus entered in the class of the most studied molecular targets in oncology [2–11]. Likewise, in the selection of an accessible target for *in vivo* imaging of the tumor microenvironment, Carbonic Anhydrase undoubtedly represents an ideal candidate. Furtheremore, it has been recently demonstrated that in breast cancer hCA IX and hCA XII exhibit distinct and non-overlapping expression patterns [24], being hCA XII high expression associated with better survival statistics, while hCA IX expression is associated with a more aggressive tumor phenotype, metastasis and resistance to therapies. Alongside this aspect, an additional reason for our focus on CAIX is the presence in its structure of an extracellular, proteoglycan-like domain (PG), which is absent in all

other forms of CAs, including CAXII. This unique structural feature of CAIX is becoming an increasingly attractive target in the development of CAIX inhibitory fragments. Indeed, the PG domain, seems to play a decisive role in supporting the CA catalytic activity and to be involved in cell-cell adhesion and intercellular communication, since both PG deletion and treatment with the PG-binding antibody M75 reduce adhesion and spreading of cancer cells [20,25]. Compared with the numerous high affinity inhibitors of the CA catalytic site, inhibitors directed against the PG region are very promising as they can provide high selectivity. Very recently it was reported that the humanized antibody CA9hu-2 against CAIX PG domain showed a high antitumoral efficacy with the absence of cross-reaction with other CAs [26].

Similarly, the development of a diagnostic imaging protocol to visualize the expression of CAIX *in vivo* by distinguishing it from other isoforms would have a huge prognostic potential. The PG-targeting based imaging techniques explored so far are predominantly Optical imaging and PET/CT, both displaying high sensitivity and thus a remarkable ability to visualize even low concentrations of targets *in vivo*. Ref. [27] reported on the use of a radiolabeled antibody, G250, for PET-CT imaging of advanced renal cancer. This clinical application showed that it was possible to visualize tumor areas with high CAIX expression, as confirmed by immunohistochemistry data.

The low availability of MRI studies is undoubtedly due to the sensitivity of the technique, which is inadequate to detect *in vivo* concentrations characteristic of this type of molecular target. On the other hand, the development of MRI imaging procedures would be strongly desirable given the low invasiveness of the technique combined to a high resolution that allows the acquisition of detailed morphological images. The strategy proposed in our study aims to overcome these limitations by using liposomal probes able of i) carrying a large amount of contrast agent per single target and ii) being up-taken into the cells with the consequent release of their content.

It is well established that entrapping a large amount of paramagnetic molecule in the core of a liposome results in a "quenching" of their T1 effect on the proton relaxation rate of bulk water. This happens because the exchange rate between the water inside and outside the liposome is lower than the relaxation rate of compartimentalized water protons. Therefore, the release of liposome payload (or the extensive disruption of the membrane structure) results in the "dequenching" of the relaxation effect, that in turn produces an increase in the MRI signal. In several studies, the "quenching" of paramagnetic agents embedded in liposomes'inner cavity has been exploited to develop probes responsive to the release of liposome contents at the site of interest [28,29]. The rationale for choosing the LIP_PepC system, loaded with a "quenched" Gd-based contrast agent solution, for imaging CAIX expression lies in the possibility to follow the fate of the probe once it reaches its destination.

In principle, the MRI approach allows to get important insights about the process associated to the binding interaction between LIP_PepC and the CAIX PG domain. First, the probe could remain linked to the outer cell membrane surface, where it gives raise to a low MRI signal. Next the liposome may degrade still in the extracellular space and this process is expected to produce a limited SE owing to the release of Gd-complex that would be quickly washed away. In another scenario the probe could be internalized, and the paramagnetic vesicle could remain intact in the intracellular medium (low SE). Finally, as shown in this study with the TS/A cells, it could be degraded intracellularly with a strong SE effect.

In fact, the analysis of the MR images acquired within a 24-hour timeframe following the end of incubation of TS/A and MDA-MB-231 cells with Lip_PEPC and non-targeting liposomes revealed a marked increase in the SE only for TS/A incubated with Lip_PEPC. These results undoubtedly demonstrated that there is a specificity toward CAIX and that the binding between the probe and the enzyme is able to induce receptor-mediated internalization, as also reported for an antibody directed against the active site of CAIX [26]. In particular, the progressive increase of signal enhancement, starting from a barely detectable contrast at t=0 ending with a final enhancement of 100 % after 24 hours allows to propose a receptor-mediated internalization mechanism after which the probe gradually releases the contrast agent, which accumulates in the intracellular medium reducing the T1 of intracellular water over time. Assuming this CAIX mediated internalization process, the low SE observed at t =0 would correspond to the integer and "quenched" probe while the increase of the

 doi:10.20944/preprints202308.1696.v1

MRI signal over time indicates that the paramagnetic solution is gradually escaping somehow from the liposomal core to the cytosol. Furthermore the concentration of Gd per cells measured by ICP enables us to calculate approximatively the number of liposomes internalized per cell, estimated to be about 6000.

The evidence presented in this study regarding the internalization of the probe and subsequent release of its contents could pave the way for the advancement of novel therapeutic approaches in anticancer drug delivery.

4. Materials and Methods

4.1. Solid phase peptide synthesis

All Fmoc-protected amino acids were purchased from Novabiochem®, and N,N-diisopropylcarbodiimide (DIC), OxymaPure®, and Fmoc-H-Rink Amide ChemMatrix resin (0.4 mmol/g) were purchased from Sigma-Aldrich Co. (Merck, St. Louis, MO, USA). Solvents for synthesis, deprotection reagents and cleavage reagents were of synthesis grade and purchased from Sigma-Aldrich Co. (Merck, St. Louis, MO, USA). Solvents and other chemicals used for high-performance liquid chromatography (HPLC) were purchased from VWR International. Peptide synthesis sequences were synthesized using a Liberty Blue™ automated microwave peptide synthesizer purchased from CEM, following a standard Fmoc protocol. The H-Rink Amide ChemMatrix resin was used as the solid support. Standard couplings of amino acids were carried out in DMF using DIC/OxymaPure® activation and piperidine deprotection. After completing synthesis, the resin with the bound peptide was moved into a reactor for washings and then cleavage. Washings were done with 100 mL of Dimethylformamide (DMF) first, then with 100 mL of Dimethyl carbonate (DMC), and finally with 25 mL x 2 of EtOEt. For drying, the reactor was connected to the vacuum pump for 1 hour. The peptide was cleaved from the resin manually by using Trifluoroacetic acid (TFA) under gentle agitation for 2 hours at room temperature in the presence of scavengers (standard cleavage solution: TFA/Phenol/MilliQWater/Triisopropyl silane (TIPS) 88:5:5:2) to avoid oxidation. After filtration, the crude peptides were precipitated by the addition of cold diethyl ether, centrifuged, washed with cold Et2O five times, dried and dissolved in ultrapure water.

Analyses of synthesized peptides were carried out by UPLC-MS Acquity H-Class Plus, on an Acquity UPLC Peptide BEH C18 column (300 Å, 1.7 µm, 2.1 mm x 100 mm), both purchased from Waters, with solvent B (acetonitrile with 0.05% TFA) versus solvent A (water with 0.05% TFA) using a 5%–95% to a 100%-0% gradient, at a flow rate of 0.4 mL/min for 13 min. Purification was performed through an HPLC AKTApurifier 10 on an X Terra Perp MS C18 OBDTM (5 µm, 19 mm x 100 mm) column in order to recover a fraction that would ensure the highest purity, and a new UPLC-MS analysis was performed. Finally, peptides were frozen, lyophilized, and stored at -20°C.

4.2. Liposomes

Liposomes were prepared using the thin-film hydration method [30]. The lipids mixture chosen for liposome synthesis was DPPC (1, 2-Dipalmitoyl-sn-glycero-3-phosphocholine), DSPE-PEG 2000 MeO (1,2-Distearoyl-sn-glycero-3-phosphoethanolamine-N-[methoxy(polyethyleneglycol)-2000], ammonium salt), DSPE-PEG 2000 Mal (1,2-distearoyl-sn-glycero-3-phosphoethanolamine-N-[maleimide(polyethylene glycol)-2000] ammonium salt) at a 95:4:1 molar ratio. All lipids were purchased from Sigma-Aldrich Co. (Merck, St. Louis, MO, USA). The total amount of phospholipids was 20 mg/mL, dissolved in chloroform, which was slowly evaporated until a thin film was formed. The lipidic film was left under vacuum until total evaporation of chloroform (2 hours) and then hydrated with a 300 mM aqueous solution (pH=6.7) of the paramagnetic complex Gd-HPDO3A (ProHance). Gd-HPDO3A (HPDO3A = 1,4,7-tris(carboxymethyl)-10-(20 -hydroxypropyl)-1,4,7,10-tetraaza-cyclododecane) is commercially available from Bracco Imaging S.p.A under the trade name of ProHance. To generate liposomes, the mixtures were sonicated using an immersion-tip instrument (SONOPULS HD 2070 Bandelin ultrasonic homogenizer, 20 KHz; Bandelin Electronic, Berlin, Germany). Sonication was performed in 2 cycles of 45 seconds each, with 30% power. The suspension

Preprints (www.preprints.org) | NOT PEER-REVIEWED | Posted: 24 August 2023 doi:10.20944/preprints202308.1696.v1

was reacted with a controlled excess of synthesized peptides to functionalize all maleimide residues present on the liposomal surface. The final suspension was purified from non-encapsulated metal complex and unbound peptide by dialysis carried out against an isotonic HEPES buffer (5 mM HEPES, 0.15 M NaCl, pH 7.4) at 4°C using dialysis cellulose membrane with 14KDa molecular weight cut-off purchased from Sigma-Aldrich, St. Louis, MO, USA. After purification, the liposome size, the mean diameter, and the polydispersity index (PDI) were determined using dynamic light scattering (DLS, Zetasizer Nano ZS, Malvern, UK) at 25°C and an angle of 90° upon diluting the liposome solution 1:100 in HEPES/NaCl buffer. The final concentration of Gd-HPDO3A in the liposome suspensions was determined by NMR magnetic susceptibility measurement, Evans assay, with a Bruker 600 MHz spectrometer (AVANCE 600, 14 T). The total amount of Gd and the size of the liposomes allowed the molar concentration of the liposomes to be determined by the following formula:

$$[Lip]M = \frac{\frac{[Gd]_{tot}}{Vol_{lip} * [Gd]_{hydr}}}{N_A}$$

where [Gd]tot is the concentration of Gadolinium in the overall liposomes suspension, [Gd]hydr is the concentration of Gadolinium in the hydration solution, used for the liposome preparation, Vol_{lip} is the volume of liposomes (in L) and N_A is the Avogadro's number.

4.3. Cell Lines and Incubation Protocol

TS/A cells (kindly provided by Prof. F. Cavallo's group, University of Turin) were cultured in L-GLUT RPMI 1640 (Euroclone) medium, supplemented with 10% (v/v) fetal bovine serum (FBS, Sigma-Aldrich, St. Louis, MO, USA) and 1% Penicillin-Streptomycin (10,000 IU/mL penicillin, 10,000 IU/mL streptomycin, Corn- Int. J. Mol. Sci. 2022, 23, 12878 12 of 18 ing Cellgro, Manassas, VA, USA). MDA-MB-231 cells (kindly provided by Prof. D. Longo's group, University of Turin) were cultured in DMEM high glucose (Euroclone) medium, supplemented with 10% (v/v) fetal bovine serum (FBS, Sigma-Aldrich, St. Louis, MO, USA), 1% (v/v) Penicillin-Streptomycin (10,000 IU/mL penicillin, 10,000 IU/mL streptomycin, Corn- Int. J. Mol. Sci. 2022, 23, 12878 12 of 18 ing Cellgro, Manassas, VA, USA), and if not present, Glutamine 4nM. These cells were maintained in a 5% CO2 incubator at 37°C until the cells attained 80% confluency and were further used for in vitro experiments. For the cell binding experiments, $1x10^6$ cells were seeded in 6 cm diameter dishes. After 24 hours, the cells were incubated with the binding solution consisting in a medium solution with a liposome concentration of 56nM, for 4 hours at 37°C and 5% CO2. At the end of the incubation, cells were washed three times with 2 mL of PBS and detached using a cell scraper. Cells were also transferred into glass capillaries for MRI analysis.

4.4. MRI analysis

Cells were placed in glass capillaries inside an agar phantom, and MR images were acquired using a standard T1-weighted multi-slice spin echo sequence (TR (repetition time)/TE (echo time)/NEX (number of excitations) = 150/3.0/8, FOV (field of view) = 10x10 mm, slice thickness = 1mm, matrix size 128 × 128) on a Bruker Avance300 spectrometer (7T) equipped with a Micro 2.5 microimaging probe (Bruker BioSpin, Ettlingen, Germany).

The Mean Signal Intensity (SI) was determined on T1w-images by manually drawing regions of interest (ROIs) inside the capillaries with ImageJ software (http://rsb.info.nih.gov/ij/). The T1 contrast enhancement (T1enh%) was calculated using the following formula:

$$SE\% = \frac{SI_{sample} - SI_{ref}}{SI_{ref}} x\ 100$$

where SI_{Sample} and SI_{ref} are signal inensities of cells incubated with the binding solution and pure medium, respectively. Each value was normalized with respect to the noise signal.

5. Conclusions

In summary, this study has demonstrated that the probe Lip_PepC shows high specificity for the CA-IX isoform with a good sensitivity threshold. These findings provide a solid basis for the preclinical translation of CAIX PG domain targeting probes in murine models. Moreover, extending a similar approach to target the CAXII isoform could allow the design of peptidic nano-vectors that selectively target either hCA IX or hCA XII isoforms in vivo, both of which are correlated with different prognostic severities in breast cancer. The determination of the expression ratio between hCA IX and hCA XII could potentially lead to the identification of a new biomarker for tumor proliferation.

Funding: The FOE contribution of the Italian Ministry of Research to the MultiModal Molecular Imaging Italian Node (www.mmmi.unito.it) of Eurobioimaging ERIC (www.eurobioimaging.eu) is gratefully acknowledged.

Data Availability Statement: we do not have a public data sharing bank to make raw data available.

Acknowledgments: In this section, you can acknowledge any support given which is not covered by the author contribution or funding sections. This may include administrative and technical support, or donations in kind (e.g., materials used for experiments).

Conflicts of Interest: The authors declare no conflict of interest. The funders had no role in the design of the study; in the collection, analyses, or interpretation of data; in the writing of the manuscript; or in the decision to publish the results.

References

1. N. Azamjah, Y. Soltan-Zadeh, e F. Zayeri, «Global Trend of Breast Cancer Mortality Rate: A 25-Year Study», Asian Pac J Cancer Prev, vol. 20, n. 7, pagg. 2015–2020, lug. 2019, doi: 10.31557/APJCP.2019.20.7.2015.
2. I. F. Robey et al., «Bicarbonate Increases Tumor pH and Inhibits Spontaneous Metastases», Cancer Res, vol. 69, n. 6, pagg. 2260–2268, mar. 2009, doi: 10.1158/0008-5472.CAN-07-5575.
3. Zheng, T., Jäättelä, M., & Liu, B. (2020). pH gradient reversal fuels cancer progression. The International Journal of Biochemistry & Cell Biology, 125, 105796.
4. Fais, S., & Marunaka, Y. (2020). The acidic microenvironment: is it a phenotype of all cancersA focus on multiple myeloma and some analogies with diabetes mellitus. Cancers, 12(11), 3226.
5. Hamaguchi, R., Isowa, M., Narui, R., Morikawa, H., & Wada, H. (2022). Clinical review of alkalization therapy in cancer treatment. Frontiers in Oncology, 12.
6. V. Alterio, A. Di Fiore, K. D'Ambrosio, C. T. Supuran, e G. De Simone, «Multiple Binding Modes of Inhibitors to Carbonic Anhydrases: How to Design Specific Drugs Targeting 15 Different Isoforms», Chem. Rev., vol. 112, n. 8, pagg. 4421–4468, ago. 2012, doi: 10.1021/cr200176r.
7. C. T. Supuran et al., «Inhibition of carbonic anhydrase IX targets primary tumors, metastases, and cancer stem cells: Three for the price of one», Med Res Rev, vol. 38, n. 6, pagg. 1799–1836, set. 2018, doi: 10.1002/med.21497.
8. A. Di Fiore, C. T. Supuran, A. Scaloni, e G. De Simone, «Post-translational modifications in tumor-associated carbonic anhydrases», Amino Acids, ago. 2021, doi: 10.1007/s00726-021-03063-y.
9. V. Alterio et al., «Biochemical and Structural Insights into Carbonic Anhydrase XII/Fab6A10 Complex», Journal of Molecular Biology, vol. 431, n. 24, pagg. 4910–4921, dic. 2019, doi: 10.1016/j.jmb.2019.10.022.
10. J. Chiche et al., «Hypoxia-Inducible Carbonic Anhydrase IX and XII Promote Tumor Cell Growth by Counteracting Acidosis through the Regulation of the Intracellular pH», Cancer Res, vol. 69, n. 1, pagg. 358–368, gen. 2009, doi: 10.1158/0008-5472.CAN-08-2470.
11. E. Langella, M. Buonanno, G. De Simone, e S. M. Monti, «Intrinsically disordered features of carbonic anhydrase IX proteoglycan-like domain», Cell. Mol. Life Sci., vol. 78, n. 5, pagg. 2059–2067, mar. 2021, doi: 10.1007/s00018-020-03697-3.
12. D. L. Longo, A. Busato, S. Lanzardo, F. Antico, e S. Aime, «Imaging the pH evolution of an acute kidney injury model by means of iopamidol, a MRI-CEST pH-responsive contrast agent: MRI-CEST pH Evolution in an AKI Mouse Model», Magn. Reson. Med., vol. 70, n. 3, pagg. 859–864, set. 2013, doi: 10.1002/mrm.24513.
13. Kunal N. Morea, et al "Acetazolamide-based [18F]-PET tracer: In vivo validation of carbonic anhydrase IX as a sole target for imaging of CA-IX expressing hypoxic solid tumors" [Bioorg. Med. Chem. Lett. 28 (5) (2018) 915–921]
14. Peng-Cheng Lv, Jyoti Roy,Karson S. Putt,and Philip S. Low "Evaluation of a Carbonic Anhydrase IX-Targeted Near-Infrared Dye for Fluorescence-Guided Surgery of Hypoxic Tumors" Mol Pharm. 2016 May 02; 13(5).

15. E. Cittadino et al., "In vivo magnetic resonance imaging detection of paramagnetic liposomes loaded with amphiphilic gadolinium(III) complexes: Impact of molecular structure on relaxivity and excretion efficiency," Chempluschem, vol. 78, no. 7, pp. 712–722, Jul. 2013, doi: 10.1002/cplu.201300096.
16. Nina Kostevšek et al,"Magneto-Liposomes as MRI Contrast Agents: A Systematic Study of Different Liposomal Formulations.Nanomaterials (Basel)". 2020 May; 10(5): 889.
17. V. P. Torchilin, «Recent advances with liposomes as pharmaceutical carriers», Nat Rev Drug Discov, vol. 4, n. 2, pagg. 145–160, feb. 2005, doi: 10.1038/nrd1632.
18. S. Aime, A. Barge, E. Gianolio, R. Pagliarin, L. Silengo, e L. Tei, «High Relaxivity Contrast Agents for MRI and Molecular Imaging», in Molecular Imaging, vol. 49, A. A. Bogdanov e K. Licha, A c. di Springer Berlin Heidelberg, 2005, pagg. 99–121. doi: 10.1007/3-540-26809-X_6.
19. Son, S., Kim, J. H., Wang, X., Zhang, C., Yoon, S. A., Shin, J., ... & Kim, J. S. (2020). Multifunctional sonosensitizers in sonodynamic cancer therapy. Chemical Society Reviews, 49(11), 3244-3261
20. A. John, M. Sivashanmugam, S. K. Natarajan, e V. Umashankar, «Computational modeling of novel inhibitory peptides targeting proteoglycan like region of carbonic anhydrase IX and in vitro validation in HeLa cells», Journal of Biomolecular Structure and Dynamics, vol. 38, n. 7, pagg. 1995–2006, mag. 2020, doi: 10.1080/07391102.2019.1623075.
21. R. Behrendt, P. White, e J. Offer, «Advances in Fmoc solid-phase peptide synthesis», J. Pept. Sci., vol. 22, n. 1, pagg. 4–27, gen. 2016, doi: 10.1002/psc.2836.
22. Daniele M. Corsi,1Carlos Platas-Iglesias,1,2Herman van Bekkum1and Joop A. Peters "Determination of paramagnetic lanthanide(III)concentrations from bulk magnetic susceptibility shiftsin NMR spectra" Magn. Reson. Chem.2001;39: 723 – 726
23. Antje Güttler, Yvonne Eiselt et al "Betulin Sulfonamides as Carbonic Anhydrase Inhibitors and Anticancer Agents in Breast Cancer Cells" International Journal of Molecular Sciences
24. D. A. Whittington et al., «Crystal structure of the dimeric extracellular domain of human carbonic anhydrase XII, a bitopic membrane protein overexpressed in certain cancer tumor cells», Proc. Natl. Acad. Sci. U.S.A., vol. 98, n. 17, pagg. 9545–9550, ago. 2001, doi: 10.1073/pnas.161301298.
25. Hilvo, M., Baranauskiene, L., Salzano, A. M., Scaloni, A., Matulis, D., Innocenti, A., ... & Parkkila, S. (2008). Biochemical characterization of CA IX, one of the most active carbonic anhydrase isozymes. Journal of Biological Chemistry, 283(41), 27799-27809.
26. Zatovicova M. et al. "Novel humanized monoclonal antibodies for targeting hypoxic human tumors via two distinct extracellular domains of carbonic anhydrase IX." Cancer Metab. 2022 Feb 2;10(1):3. doi: 10.1186/s40170-022-00279-8.).
27. Pryma DA, O'Donoghue JA, Humm JL, Jungbluth AA, Old LJ, Larson SM, Divgi CR. "Correlation of in vivo and in vitro measures of carbonic anhydrase IX antigen expression in renal masses using antibody 124I-cG250." J Nucl Med. 2011 Apr;52(4):535-40. doi: 10.2967/jnumed.110.083295. Epub 2011 Mar 18. PMID: 21421715
28. Paula ENZIAN, Elisabeth KIRCHERT, Nina KLEINEBERG, Christian SCHELL, Ramtin RAHMANZADEH, "Light-Induced Permeabilization of Liposomes with a new Porphyrin and its Chlorin and Bacteriochlorin, Photodiagnosis and Photodynamic Therapy" Volume 41, 2023, 103483,
29. Silvia Rizzitelli; Pierangela Giustetto,; Juan C Cutrin, Daniela Delli Castelli,.; Cinzia Boffa,.; Marta Ruzza,.; Valeria Menchise; Filippo Molinari; Silvio Aime; Enzo Terreno. ": Preclinical in vivo MRI-guided visualization of Doxorubicin release from liposomes stimulated by pulsed low intensity non-focused Ultrasound" Release. 2015 Mar 28;202:21-30. doi:10.1016/j.jconrel.2015.01.028
30. J. Lasch, V. Weissig, M. Brandl, Preparation of liposomes, in:V.P. Torchilin, V. Weissig (Eds.), Liposomes, Oxford University Press, New York, 2003, pp. 3–27.